MORPHOLOGICAL, HISTOPATHOLOGICAL AND SECONDARY STRUCTURE ANALYSIS OF SECOND INTERNAL TRANSCRIBED SPACER (ITS-2) REGION OF *Gigantocotyle explanatum* (TREMATODA: PARAMPHISTOMIDAE) IN BUFFALOES OF PAKISTAN

Muhammad Arshad[1], Kiran Afshan[1,*], Humair Hayat[1], Sabika Firasat[1], Imtiaz Ahmad Khan[2] and Ghulam Narjis[3]

Received: 18 January 2020
Accepted: 15 March 2022

ABSTRACT

Liver infections due to amphistomes in buffaloes cause significant economic losses in livestock sector. The present study investigated the classical morphological features of adult amphistomes combined with histopathology and molecular identity in slaughtered buffaloes from Khyber Pakhtunkhwa, Pakistan. Adult amphistome were collected and morphologically characterized as *Gigantocotyle explanatum*. Morphometric measurement (n=50) were obtained with 12.05±1.68 mm in length and 5.77±0.81 mm in width, and the values of sagittal section was 6.35±1.03 x 2.98±0.50 mm in size. Severe bile duct pathology was observed with fibrosis of the duct wall with an irregular epithelial border, hyperplasia and inflammatory response with numerous neutrophils and eosinophils. The molecular identity of *G. explanatum* within Paramphistomidae was confirmed by ITS-2 rDNA sequences phylogenetic analysis based on maximum likelihood method. The genetic data based on ITS-2 secondary structure of *G. explanatum* consisted of four helix, Helix I, II and IV were conserved as compared with other closely related reference taxa of family Paramphistomidae and Gastrothylacidae. Helix III expressed some variations. The study concluded that rDNA ITS-2 and secondary structure information provides a guide for other researchers to determine the molecular taxonomic position of Paramphistomidae trematodes, data will support future clinical studies and control measures to reduce the amphistomiasis in buffaloes.

Keyword: *Bubalus bubalis*, buffaloes, *Gigantocotyle explanatum*, histopathology, molecular characterization, Pakistan

INTRODUCTION

Members of the Paramphistomidae family (Fischoeder, 1901) commonly known as amphistomes are composed of over 70 species in 19 genera (Jones, 2005). Most of these species cause

[1]Department of Zoology, Faculty of Biological Sciences, Quaid-i-Azam University, Islamabad, Pakistan, *E-mail: kafshan@qau.edu.pk

[2]Department of Veterinary Pathology, Faculty of Veterinary and Animal Sciences, Pir Mehr Ali Shah-Arid Agriculture University, Rawalpindi, Pakistan

[3]Department of Statistics, Faculty of Natural Sciences, Quaid-i-Azam University, Islamabad, Pakistan

serious infection in large ruminants that leads to high morbidity rate. However, amphistomes of genus *Gigantocotyle* parasitize the bile ducts and intrahepatic ductules of animals producing granulomatous nodules at attachment site with fibrosis and thickening of the bile ducts (Mazahery *et al*., 1994; Haque *et al*., 2011; Malik *et al*., 2017). Studies also reported histopathological alteration at the worm attachment site like inflammatory cells surround granulomatous nodules (Haque *et al*., 2011). Economic losses caused by *Gigantocotyle* are in terms of reduced growth rate, decrease in milk and meat production and increased mortality rate in affected animals.

Previously, *G. explanatum* has been identified in slaughtered buffalos in countries like Iran, India and Myanmar (Mazahery *et al*., 1994; Ichikawa *et al*., 2013). The overall distribution of tis fluke in Pakistan is still in early stages and 17.39 to 44.44% prevalence is reported from various districts of Punjab (Iqbal *et al*., 2014). Mode of natural infection by *G. explanatum* is sporadic and fresh water snail *Gyraulus convexiculus* serves as intermediate host (Naeem *et al*., 2014). True species identity of Paramphistomatidae flukes by morphological examination can be imprecise, if not performed by experienced hands due to their similar morphology while molecular speciation methods are seldom used (Chaudhry *et al*., 2017). The rDNA ITS-2 is a very useful marker for correct identification of species and have been used for many Paramphistomaetidae including *G. explanatum* (Chaudhry *et al*., 2017; Ichikawa *et al*., 2013), Fasciolidae (Chaudhry *et al*., 2015; Itagaki and Tsutsumi, 1998) and Dicrocoeliidae (Gorjipoor *et al*., 2015). The ITS-2 markers are highly conserved and can be used to differentiate the closely related taxa that have diverged very recently i.e. <50 million years ago (Mas-Coma *et al*., 2009). Addition of ITS-2 secondary structure improves the accuracy and minimize the robustness of phylogenetic tree reconstruction (Keller *et al*., 2010). In current study we combine the classical morphological identification methods along with histopathology of *G. explanatum*. Molecular characterization was under taken based on ITS-2 ribosomal DNA sequences secondary structure analysis for rapid and reliable screening of amphistome species.

MATERIALS AND METHODS

Adult fluke collection

We identified the central abattoir at Khyber Pakhtunkhwa province (34.95º N 72.33º E) of Pakistan where we projected a high prevalence of Paramphistomatidae in buffaloes. Infected bile ducts were collected soon after slaughtering, washed several times in phosphate buffer solutions (PBS) and then dissected to reveal the flukes in the biliary ducts. Amphistomes were preserved in 70% ethanol for molecular analysis and infected tissue were preserved in 10% formalin respectively. Sampling period comprised of 7 months from august 2017 to the last week of February 2018.

Morphometric Analysis

Morphometric measurements was undertaken according to existing keys (Eduardo, 1937) and were recorded for whole mount and sagittal section. Morphometric findings from the current study were compared with already reported measurements (Ichikawa *et al*., 2013; Chaudhry *et al*., 2017; Malik *et al*., 2017).

Pathological examination

Infected bile duct specimens with

Gigantocotyle parasites were preserved in 10% buffered formalin for the histopathological investigation. The tissues were sectioned stained with haematoxylin and eosin as per standard procedure described by (Slaoui and Fiette, 2011). Images were taken with digital camera (Cannon, japan) and photo plates were prepared by using Adobe Photoshop (Version 11.0; Microsoft Inc. USA). The gross pathological changes were analyzed and recorded.

Molecular analysis

Genomic DNA extraction, PCR amplification and sequence analysis

DNA was extracted from adult flukes preserved in 70% ethanol using Phenol-Chloroform method described by (Barker, 1998). DNA fragments of ITS-2 region were amplified by using universal forward primer (F=GGTGGATCACTCGGCTCGTG and reverse primer (R=TTCCTCCGCTTAGTGATATGC). The 25 µl volume of every PCR reactions comprises sample DNA (2.0 µl), buffer (2.5 µl), PCR water (14.7 µl), $MgCl_2$ (2.0 µl), primers (0.5 µl each), Taq Polymerase (0.3 µl) and 2.5 µl of dNTPs were amplified: Initial denaturation at 95ºC for 45 seconds followed by 35/ 95ºC for 45 seconds, 61 for 45 seconds and 72º with a final extension for 10 minutes. Sequencing was performed at (CAMB) Center for Applied Molecular Biology University of Punjab Pakistan. Chromatograms were inspected in Chromas for error or ambiguity before undertaking further analysis.

Phylogenetic analysis and secondary structure prediction

Phylogenetic analysis were performed by using MEGA7 (Kumar *et al*., 2016), through Maximum Likelihood method. A total of 44 nucleotide sequences involved and bootstrap supports were taken based on 1000 replicates. ITS-2 sequences of *Haemonchus contortus* (KX829170) and *Caenorhabditis elegans* (JN636101) were used as outgroup to root the trees.

The secondary structures of ITS-2 were predicted by comparing RNA folding patterns with (*Paramphistomum cervi*, *Gastrothylax crumenifer* and *Calicophoron calicophorum*) by using Mfold ver. 3 (Zuker, 2003) with default parameters. Set the temperature at 37ºC. Mfold generated with several alternative folding patterns for each most stable ITS-2 secondary structure having same minimal energy values.

RESULTS AND DISCUSSION

Morphometric characterization

The morphometric values of adult *G. explanatum* are summarized in Table 1. Identification was carried out based on the shape and position of testes, Oesophagus, uterus, round ventral sucker (acetabulum). We have described the morphology of Paramphistomatidae flukes as described by Eduardo (1937). Measurements of the whole mount of worm (Figure 1) were about 12.05±1.68 mm in length and 5.77±0.81 mm in width, with diagonal testis. The values of present study were found very much close to the findings of Chaudhry *et al*. (2017) as they described length as 10.00 to 11.9 mm and width 4.3 to 5.8 mm, but slightly larger than the findings of other related studies (Ichikawa *et al*., 2013; Malik *et al*., 2017).

Histopathological examination of bile duct

Severe bile duct pathology was observed with atrophied, clearly visible granulomatous nodules on epithelium, obstruction at the site of

attachment by means of acetabulum, consistent with previous reports of *G. explanatum* infection in domestic buffalo (Ichikawa *et al*., 2013; Mazahery *et al*., 1994; Chaudhry *et al*., 2017). Cross section of the bile duct showed the attachment plug formed because of the powerful sucking of the amphistomes (Figure 2), small nodule, dilated blood vessels, glandular infiltration and intrusion of inflammatory cells in the nodular region. Mucosal proliferated hyperplasia formed villi like structures in lumen of the bile duct. Similarly the hyperplasia and hypertrophy of mucosa of bile ducts with fibrosis is also reported in other studies (Khatoon *et al*., 2003; Ahmedullah *et al*., 2007; Malik *et al*., 2017). Gamit *et al*. (2017) support the findings that complete blockage of ducts occur due to mucosal attachment of *G. explanatum*. Thickening and fibrosis of sub mucosa along colored nodules is also reported. Present study correlates with the recent study of Gumasta *et al.* (2020) in India who reported pathogenicity of *G. explanatum* in the bile duct and hemorrhages at attachment sites with high rate of infection and liver's bluish color.

Molecular analysis

Phylogenetic tree based on ITS-2 sequences revealed that present *G. explanatum* from Pakistan is closely related with amphistomes species of China, India, Myanmar, and Bangladesh. (Figure 3). Furthermore the isolates found in India showed same clade with the haplotypes from Bangladesh and Nepal (Laidemitt *et al*., 2017; Hayashi *et al*., 2016. This may explained that these countries have same geography, similar culture and migration of animals (Mohanta *et al*., 2014). The genetic distance matrix was generated and (Table 2) showed values less than 0.022 which confirmed the closeness to sister species. The genetic distance of *E. explanatum* with India, Myanmar, Bangladesh and China was recorded as in the rage of 0.00 to 0.004. Studies conducted on species with genetic distance <1.3% (0.013) are placed in same clade and the value with >6.5% (0.065) are rooted at different clades (Laidemitt *et al*., 2017).

Secondary structure model of ITS2

Predicted secondary structures for the ITS2 region of *G. explanatum* of present study with three reference species analysed using Mfold, resulted in a four-helix model with unpaired central core. The paired region was with double helix form and the unpaired regions with loops and bulges (Figure 4). The secondary structure of *G. explanatum* compared with other members of family Paramphistomidae and Gastrothylacidae, showed that the Helix I, II and IV were highly conserved with no variations. Helix III expressed some variations i.e. it contained 59 paired nucleotides with four (4) bulges and one (1) apical loop in case of *G. explanatum*. Two AA and one UU mismatches are present in all the given structures of parasites in Helix-III and Helix-IV respectively. The UU mismatch of helix-II is identical in all except *C. calicophorum*. Helix III was the longest and contained a UGGU motif 5" to the apex. This is identical as predicted by (Coleman, 2007). The folding ability of ITS-2 sequences of species and genera of a family are compared to identify the conserved regions and discover a structure which is common to all of them. Moreover, secondary structure prediction is vital for the alignment of ITS-1 and ITS-2 (Mai and Coleman, 1997). Schultz *et al.* (2005) described different hallmarks for the structure of ITS-2, which are including the four helices with longest Helix III, different motives like UGGGU, UGG or GGU and a UU mismatch in Helix II. These accumulation of secondary structures, their variant conformation should

Table 1. Morphometric measurements (mm) with Mean (±) Standard Deviation (±) of n=50 adult *Gigantocotyle explanatum* in buffaloes of Khyber Pakhtunkhwa, Pakistan.

Adult measurements (mm)	**Whole mount**	**Standard measurements**	**Sagittal section**	**Standard measurements**
Body length (BL)	12.05±1.68	10.84-18.39 (Devi *et al*., 2017)	6.35±1.03	7.65±1.25 (Sadaf *et al*., 2017)
Body width (BW)	5.77±0.81	5.01-7.32	2.98±0.50	3.47±0.63
Acetabulum diameter min	3.23±0.41	1.46-1.80	1.40±0.35	2.47±0.64
Acetabulum diameter max	3.45±0.46	1.62-4.52	1.98±0.42	3.24±0.57
Pharynx length (PL)	1.19±0.25	0.62-0.90	0.90±0.23	0.86±0.11
Pharynx width (PW)	1.33±0.28	1.04±0.13	0.86±0.26	0.67±0.13
Oesophagous length (Oes L)	0.69±0.14	0.45-0.72	-	-
Intestinal caeca length (InL)	6.88±0.30	8.98±1.15	-	-
Anterior testis length (T1)	2.81±0.21	0.20-0.50	1.30±0.21	1.06±0.29
Anterior testis width (T1W)	3.04±0.32	0.20-0.50 (Sadaf *et al*., 2017)	1.35±0.31	1.80±0.45
Posterior testis length (T2L)	2.95±0.18	2.24±0.45	1.37±0.16	1.80±0.45
Posterior testis width (T2W)	3.27±0.18	4.31±1.00	1.53±0.17	1.82±0.56
Ovary length (Ov L)	0.28±0.09	(0.14 mm)	0.44±0.18	0.42±0.15
Ovary width (Ov W)	0.39±0.10	0.30±0.06	0.44±0.16	0.36±0.1
Mehli's gland length (MGL)	0.29±0.03	0.26±0.06	-	-
Mehli's gland width (MGL)	0.20±0.03	0.20±0.04	-	-

Table 2. Estimates of Evolutionary Divergence between Sequences. Analyses were conducted using the Maximum Composite Likelihood model (Tamura *et al*., 2004). All positions containing gaps and missing data were eliminated. There were a total of 214 positions in the final dataset.

Species	Accession no.	Country	1	2	3	4	5	6	7	8	9	10	11	12	13	14	15
G. explanatum	Present study	Pakistan															
E. explanatum	AB743577	Myanmar	0.000														
E. explanatum	LC101683	Bangladesh	0.000	0.000													
E. explanatum	KF564869	India	0.004	0.004	0.004												
E. explanatum	KT198990	China	0.004	0.004	0.004	0.008											
E. explanatum	KC503920	India	0.000	0.000	0.000	0.004	0.004										
E. explanatum	JX678250	India	0.022	0.022	0.022	0.027	0.027	0.022									
P. cervi	KU365321	India	0.022	0.022	0.022	0.026	0.026	0.022	0.027								
P. epiclitum	KX840345	India	0.026	0.026	0.026	0.031	0.031	0.026	0.031	0.022							
P. leydeni	KX274232	Croatia	0.013	0.013	0.013	0.017	0.017	0.013	0.022	0.026	0.031						
F. hepatica	EF612481	Iran	1.553	1.553	1.553	1.564	1.553	1.553	1.489	1.543	1.595	1.596					
D. dendriticum	AB367789	Japan	2.290	2.290	2.290	2.304	2.290	2.290	2.174	2.206	2.248	2.251	1.827				
C. daubneyi	KT182100	South Africa	0.032	0.032	0.032	0.037	0.037	0.032	0.032	0.027	0.042	0.027	1.511	2.164			
C. calicophorum	JX678259	India	0.022	0.022	0.022	0.026	0.026	0.022	0.027	0.000	0.022	0.026	1.543	2.206	0.027		
G. crumenifer	KX840346	India	0.009	0.009	0.009	0.013	0.013	0.009	0.013	0.013	0.017	0.013	1.585	2.248	0.023	0.013	
H. contortus	KX829170	Iran	4.750	4.750	4.750	4.728	4.750	4.750	4.791	4.728	4.661	4.813	5.126	5.109	4.873	4.728	4.684

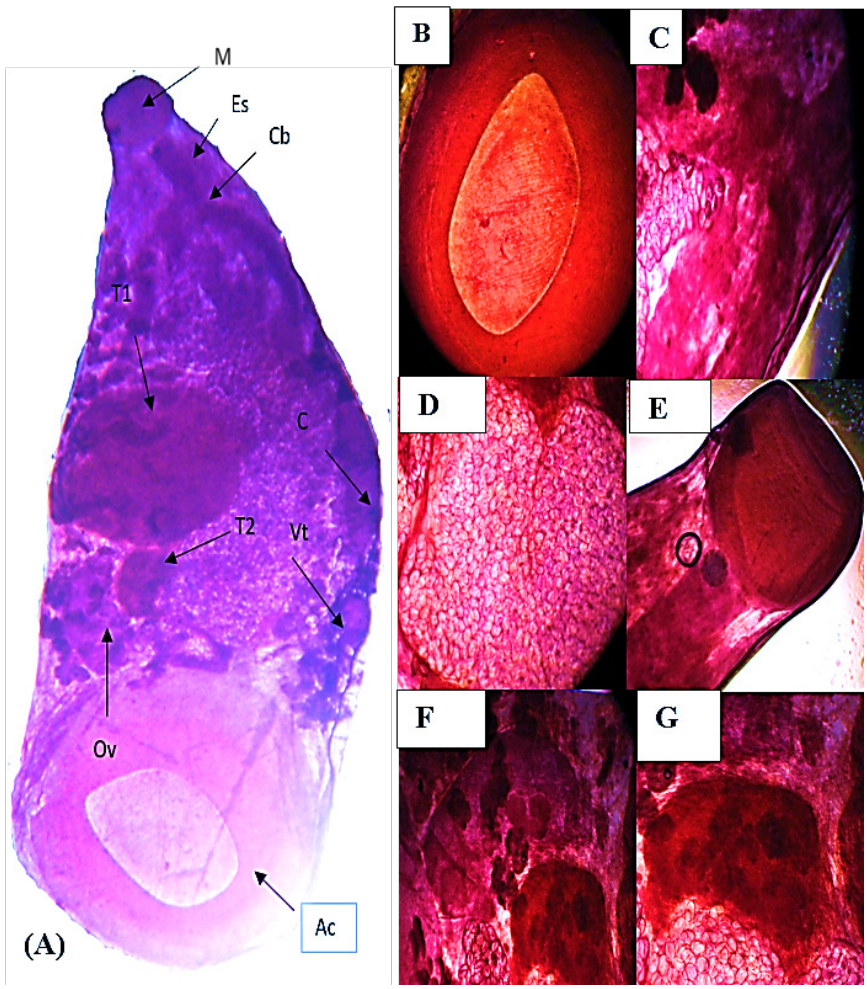

Figure 1. A, Representative whole mount of *G. explanatum* indicates M, mouth; Es, esophagus; Cb, caecum bifurcation; T1, anterior testis; T2, posterior testis; Ov, ovary; A, acetabulum; Vt, vittelaria; C, caecum. B, separate image of acetabulum; C, caecal bifurcation; D, Caecum; E, mouth with esophagus; F, testis; G, Ovary.

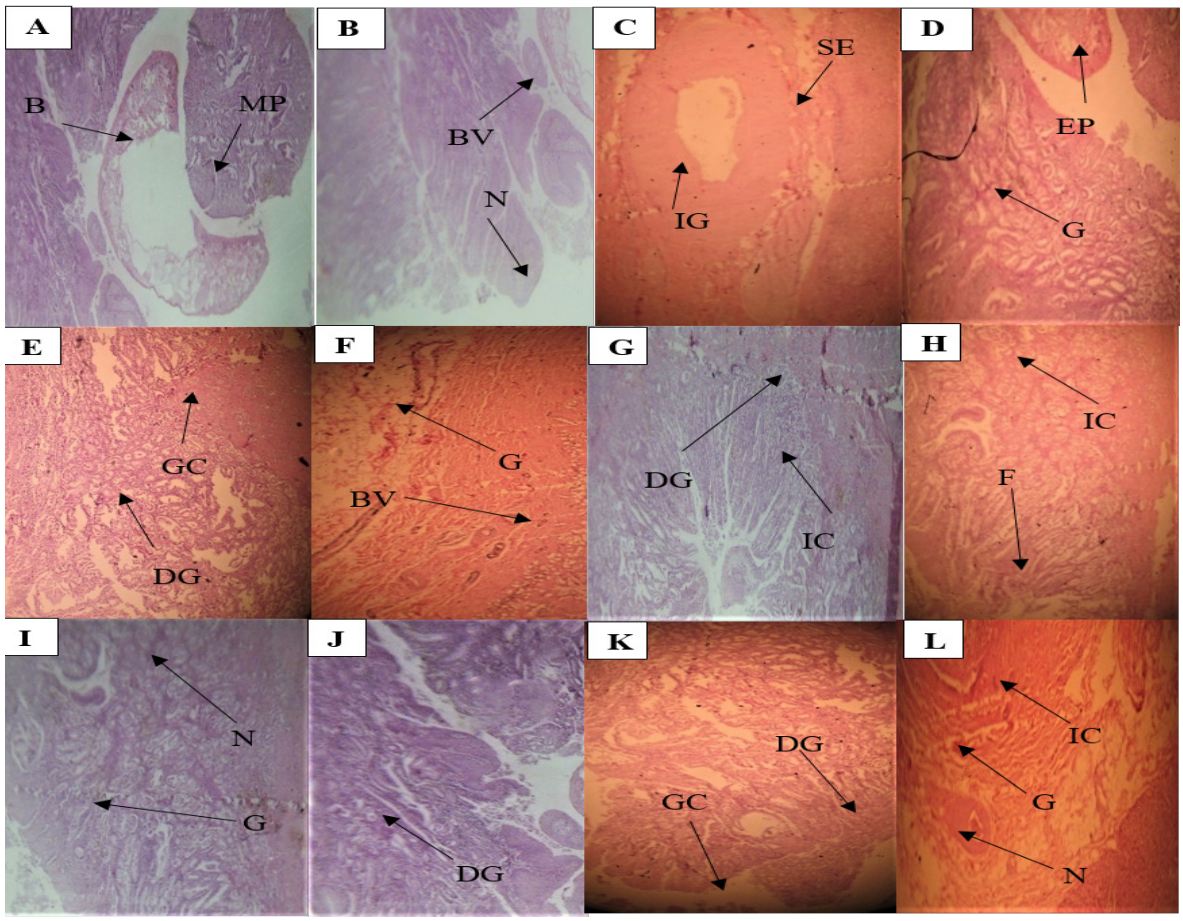

Figure 2. Histopathological examination of biliary duct, there is evident fibrosis of the duct wall with an irregular epithelial border, hyperplasia surrounded by fibrosis and inflammatory response with numerous neutrophils and eosinophils, which is typical of large bile duct obstruction. MP: mucosal plug, B: mucosal plugs formed due to parasite attachment, BV: blood vessel, N: nodule; IG: inflamed glands, SE: serosa, EP: epithelial layers, G: gland, DG: degenerated gland, GC: glandular cells, IC: inflammatory cells, F: fibrosis.

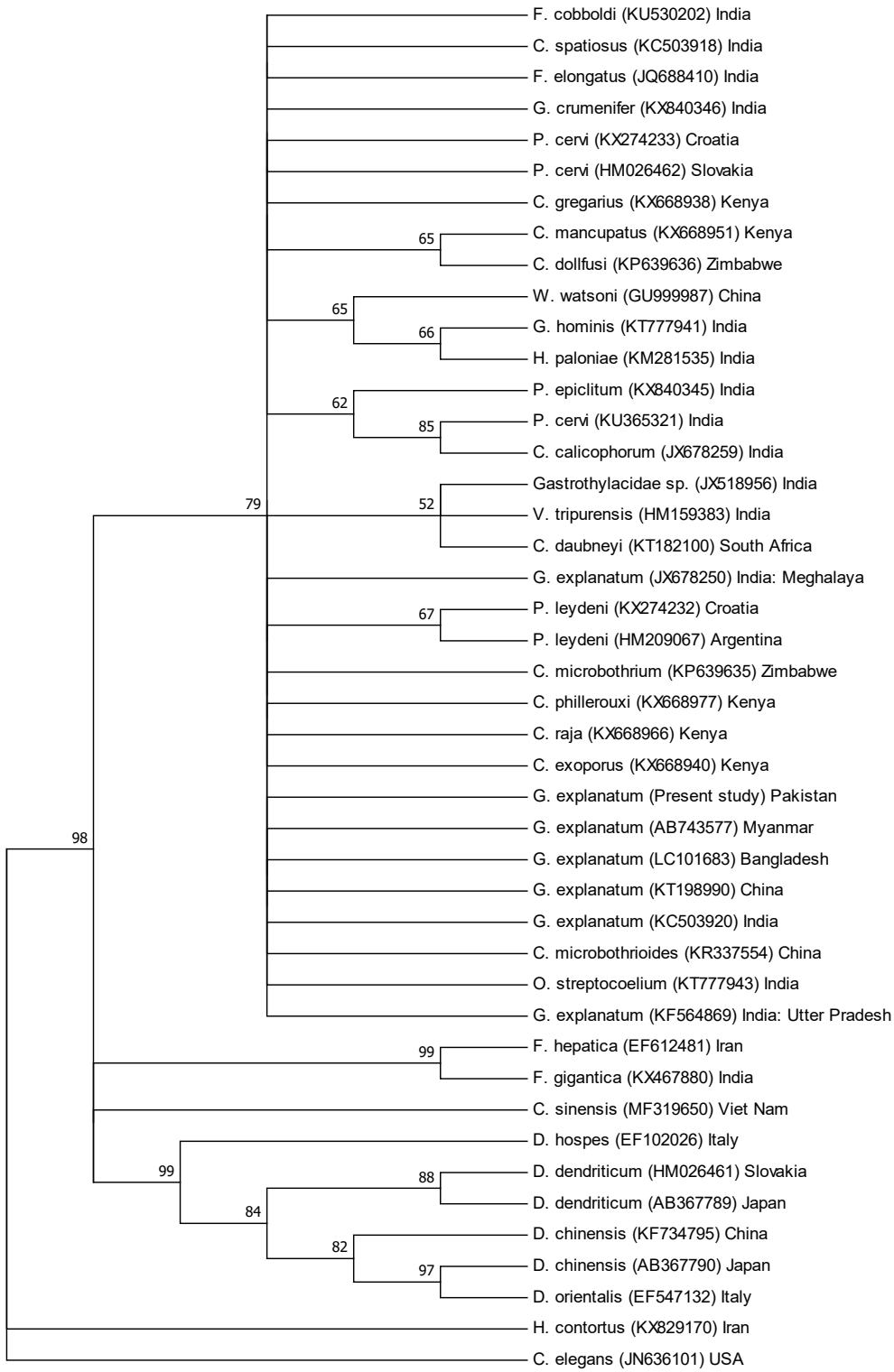

Figure 3. Molecular Phylogeny based on rDNA ITS-2 sequence data. Numbers represent bootstrap values from 1000 replicates (neighbour joining). Bootstrap values of <50% are not shown.

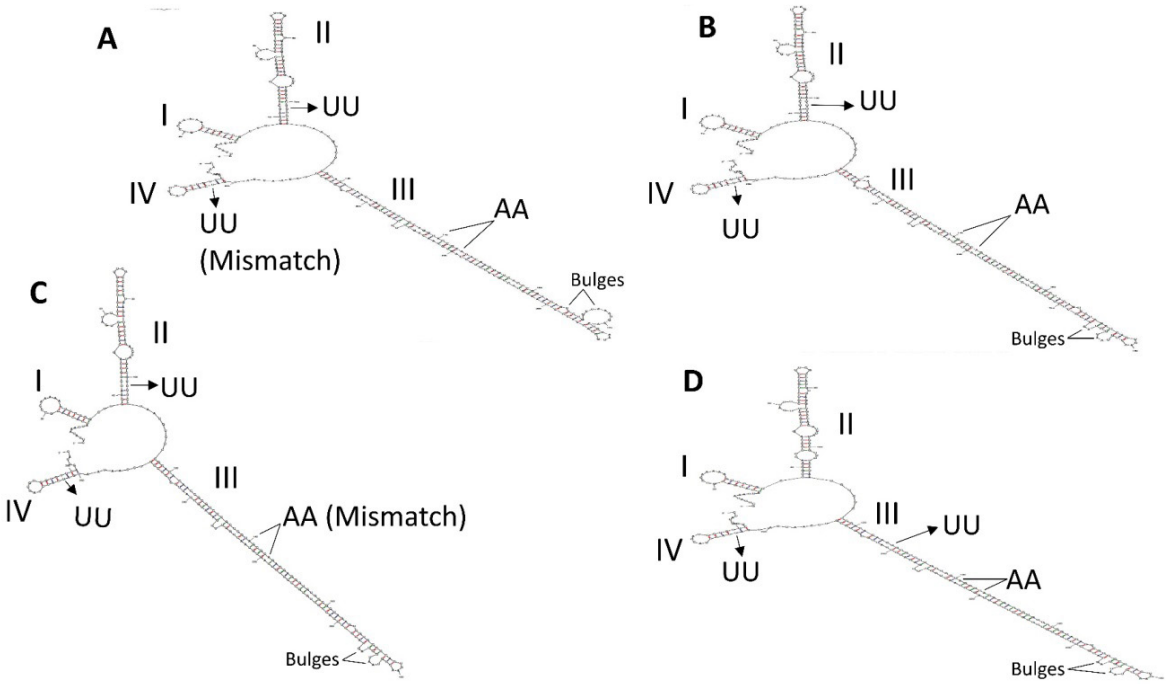

Figure 4. Predicted Secondary structures of ITS-2 of family Paramphistomidae and Gastrothylacidae based on minimum free-energy modelling using Mfold software. A) *Gigantocotyle explanatum* (free energy ΔG= -117.50 kcal/mol) B) *Paramphistomum cervi* (ΔG= -118 kcal/mol) C) *Gastrothylax crumenifer* (ΔG= -119.10 kcal/mol) D) *Calicophoron calicophorum* (ΔG= -117.70).

eventually contribute information worthy useful to student of evolution of RNA processing in different taxonomic level (Michot *et al*., 1999; Joseph *et al*., 1999).

In conclusion the morphological and secondary structure analysis confirmed the identity of *G. explanatum* in buffaloes of Pakistan. The result revealed typical bile duct obstruction with fibrosis of the duct wall with an irregular epithelial border, hyperplasia surrounded by fibrosis and inflammatory response with numerous neutrophils and eosinophils.

REFERENCES

Ahmedullah, F., M. Akbor, M.G. Haider, M.M. Hossain, M.A.H.N.A. Khan, M.I. Hossain and I.S. Shanta. 2007. Pathological investigation of liver of the slaughtered buffaloes in Barisal district. *Bangladesh Journal of Veterinary Medicine*, **5**(1&2): 81-85. DOI: 10.3329/bjvm.v5i1.1321

Barker, D.J. 1998. In utero programming of chronic disease. *Clin. Sci*., **95**(2): 115-128.

Chaudhry, U., B. van Paridon, M. Lejeune, M.Z. Shabbir, M.I. Rashid, K. Ashraf and N. Sargison. 2017. Morphological and molecular identification of *Explanatum explanatum* in domestic Water buffalo in Pakistan. *Veterinary Parasitology: Regional Studies and Reports*, **8**: 54-59. DOI: 10.1016/j.vprsr.2017.02.002

Chaudhry, U., B. van Paridon, M.Z. Shabbir, M. Shafee, K. Ashraf, T. Yaqub and J. Gilleard. 2015. Molecular evidence shows that the liver fluke *Fasciola gigantica* is the predominant Fasciola species in ruminants from Pakistan. *J. Helminthol*., **90**(2): 206-213. DOI: 10.1017/S0022149X15000176

Coleman, A.W. 2007. Pan-eukaryote ITS2 homologies revealed by RNA secondary structure. *Nucleic Acids Res*., **35**(10): 3322-3329. DOI: 10.1093/nar/gkm233

Eduardo, S.L. 1937. The taxonomy of the family Paramphistomidae with special reference to the morphology of species occurring in ruminants. *Syst. Parasitol*., **5**: 25-79.

Gamit, A.B., P.K. Nanda, R. Bhar and S. Bandyopadhyay. 2017. *Explanatum explanatum* infection in the liver of Water buffalo : A slaughter house report. *International Journal of Science, Environment and Technology*, **6**(2): 1231-1235. Available on: https://www.ijset.net/journal/1671.pdf

Gorjipoor, S., M. Moazeni and H. Sharifiyazdi. 2015. Characterization of *Dicrocoelium dendriticum* haplotypes from sheep and cattle in Iran based on the internal transcribed spacer 2 (ITS-2) and NADH dehydrogenase gene (nad1). *J. Helminthol*., **89**(2): 158-164. DOI: 10.1017/S0022149X13000679

Gumasta, P., D.K. Jolhe, R.C. Ghosh, M.K. Pandey, S.K. Patel and S. Argade. 2020. Patho-morphological study of *Gigantocotyle* spp. infection in water buffaloes (*Bubalus bubalis*). *J. Anim. Res*., **9**(4): 533-536. DOI: 10.30954/2277-940X.04.2019.6

Haque, M., C. Mohan and I. Ahmad. 2011. Natural trematode infection in liver of water buffalo (*Bubalus bubalis)*: Histopathological investigation. *Journal of Parasitic Diseases*, **35**(1): 50-53. DOI: 10.1007/s12639-011-0022-y

Hayashi, K., U.K. Mohanta, Y. Ohari, T. Neeraja, T.S. Singh, H. Sugiyama and T. Itagaki. 2016. Molecular characterization and

phylogenetic analysis of *Explanatum explanatum* in India based on nucleotide sequences of ribosomal ITS2 and the mitochondrial gene nad1. *J. Vet. Med. Sci*., **78**(11): 1745-1748. DOI: 10.1292/jvms.16-0252

Ichikawa, M., D. Kondoh, S. Bawn, N.N. Maw, L.L. Htun, M. Thein and T. Itagaki. 2013. Morphological and molecular characterization of *Explanatum Explanatum* from cattle and buffaloes in Myanmar. *J. Vet. Med. Sci*., **75**(3): 309-314. DOI: 10.1292/jvms.12-0389

Iqbal, M.N., A. Muhammad, A.A. Anjum, K.A. Shahzad, M.A. Ali and S. Ali. 2014. Epidemiology of *Gigantocotyle explanatum* in naturally infected buffaloes. *Veterinaria*, **1**(1): 15-18. Available on: http://thesciencepublishers.com/veterinaria/files/3-201402073-RV%20Final.pdf

Itagaki, T. and K.I. Tsutsumi. 1998. Triploid form of Fasciola in Japan: Genetic relationships between *Fasciola hepatica* and *Fasciola gigantica* determined by ITS-2 sequence of nuclear rDNA. *Int. J. Parasitol*., **28**(5): 777-781. DOI: 10.1016/s0020-7519(98)00037-x

Jones, A. 2005. Superfamily paramphistomoidea Fischoeder, 1901. p. 221-327. *In* Jones, A., R.A. Bray and D.I. Gibson (eds.) *Keys to The Trematoda*, Wallingford, CABI Publishing, London, UK.

Joseph, N., E. Krauskopf, M.I. Vera and B. Michot. 1999. Ribosomal internal transcribed spacer 2 (ITS2) exhibits a common core of secondary structure in vertebrates and yeast. *Nucleic Acids Res*., **27**(23): 4533-4540. DOI: 10.1093/nar/27.23.4533

Keller, A., F. Förster, T. Müller, T. Dandekar, J. Schultz and M. Wolf. 2010. Including RNA secondary structures improves accuracy and robustness in reconstruction of phylogenetic trees. *Biol. Direct*, **5(**1): 4. DOI: 10.1186/1745-6150-5-4

Khatoon, N., M.B. Fatima and M. Samreen. 2003. Histopathological changes in the liver of buffaloes by digenetic trematode Paramphistomum cervi. *Pakistan Journal of Biological Sciences*, **6**(17): 1540-1543. DOI: 10.3923/pjbs.2003.1540.1543

Kumar, S., G. Stecher and K. Tamura. 2016. MEGA7: Molecular evolutionary genetics analysis version 7.0 for bigger datasets. *Mol. Biol. Evol*., **33**(7): 1870-1874. DOI: 10.1093/molbev/msw054

Laidemitt, M.R., E.T. Zawadzki, S.V. Brant, M.W. Mutuku, G.M. Mkoji and E.S. Loker. 2017. Loads of trematodes: Discovering hidden diversity of paramphistomoids in Kenyan ruminants. *Parasitology*, **144**(2): 131-147. DOI: 10.1017/S0031182016001827

Mai, J.C. and A.W. Coleman. 1997. The internal transcribed spacer 2 exhibits a common secondary structure in green algae and flowering plants. *J. Mol. Evol*., **44**(3): 258-271. DOI: 10.1007/pl00006143

Malik, S.I., K. Afshan and M. Qayyum. 2017. Phenotyping of amphistomes, and pathological, hematological and bile biochemical response to *Gigantocotyle explanatum* infection in buffaloes. *Pak. J. Zool*., **49**(30): 979-987. DOI: 10.17582/journal.pjz/2017.49.3.979.987

Mas-Coma, S., M.A. Valero and M.D. Bargues. 2009. Chapter 2 fasciola, lymnaeids and human fascioliasis, with a global overview on disease transmission, epidemiology, evolutionary genetics, molecular epidemiology and control. *Adv.*

Parasit., **69**: 41-146. DOI: 10.1016/S0065-308X(09)69002-3

Mazahery, Y., J. Razmyar and N. Hoghooghi-Rad. 1994. *Explanatum explanatum* (Creplin, 1847) Fukui, 1929, in buffaloes in the Ahwaz area, southwest Iran. *Vet. Paraitol*., **55**(1-2): 149-153. DOI: 10.1016/0304-4017(94)90066-3

Michot, B., N. Joseph, S. Mazan, J.P. Bachellerie, L. De Biologie, M. Eucaryote and T. Cedex. 1999. Evolutionarily conserved structural features in the ITS2 of mammalian pre-rRNAs and potential interactions with the snoRNA U8 detected by comparative analysis of new mouse sequences. *Nucleic Acids Res*., **27**(11): 2271-2282. DOI: 10.1093/nar/27.11.2271

Mohanta, U.K., M. Ichikawa-Seki, T. Shoriki, K. Katakura and T. Itagaki. 2014. Characteristics and molecular phylogeny of Fasciola flukes from Bangladesh, determined based on spermatogenesis and nuclear and mitochondrial DNA analyses. *Parasitol. Res*., **113**(7): 2493-2501. DOI: 10.1007/s00436-014-3898-5

Schultz, J., S. Maisel and D. Gerlach. 2005. A common core of secondary structure of the internal transcribed spacer 2 (ITS2) throughout the Eukaryota. *RNA*, **11**(4): 361-364. DOI: 10.1261/rna.7204505

Zuker, M. 2003. Mfold web server for nucleic acid folding and hybridization prediction. *Nucleic Acids Res*., **31**(13): 3406-3415. DOI: 10.1093/nar/gkg595